Journal of Sound and Vibration (1990) **138**(1), 115-134

NATURAL MODES OF BERNOULLI–EULER BEAMS WITH SYMMETRIC CRACKS

M.-H. H. SHEN AND C. PIERRE

Department of Mechanical Engineering and Applied Mechanics, The University of Michigan, Ann Arbor, Michigan 48109-2125, *U.S.A.*

(*Received* 8 *February* 1989, *and in revised form* 14 *July* 1989)

An approximate Galerkin solution to the one-dimensional cracked beam theory developed by Christides and Barr for the free bending motion of beams with pairs of symmetric open cracks is suggested. The series of comparison functions considered in the Galerkin procedure consists of the mode shapes of corresponding uncracked beam. The number of terms in the expansion is determined by the convergence of the natural frequencies and confirmed by studying the stress concentration profile near the crack. This approach allows the determination of the higher natural frequencies and mode shapes of the cracked beam. It is found that the Christides and Barr original solution was not fully converged and that cracks render the convergence of the Galerkin's procedure very slow by affecting the continuity characteristics of the solution of the boundary value problem. To validate the theoretical results, a two-dimensional finite element approach is proposed, which also allows one to determine the parameter that controls the stress concentration profile near the crack tip in the theoretical formulation without requiring the use of experimental results. Very good agreement between the theoretical and finite element results is observed.

1. INTRODUCTION

The stress state σ_{ij} near a crack tip has the well known formulation [1, 2]

$$\sigma_{ij} = (K/\sqrt{r}) f_{ij}(\theta), \tag{1}$$

where K is the stress intensity factor, r the distance from the crack tip, and $f_{ij}(\theta)$ a set of functions of the orientation angle (a list of nomenclature is given in Appendix B). It follows from equation (1) that near a crack tip stresses are concentrated and thus local deformations occur, resulting in a reduction of the bending stiffness locally. In turn, this additional flexibility alters the global dynamics of the structure.

The knowledge of the modes of vibration of a damaged structure is useful in order to determine the location and size of cracks. For example, vibration monitoring systems can diagnose the loss of integrity of a structural member by detecting changes in its frequencies and mode shapes. The position of the damage (e.g., cracks) could be indicated without dismantling the structure and, most importantly, such crack monitoring could even be performed on line [3]. Thus, the use of vibration measurement and analysis for monitoring structural integrity is a viable crack detection technique [3-6]. This motivates the analysis of the dynamics of cracked structures.

Stress concentrations render the analysis of cracked structures difficult. Typically, the crack-tip section is modeled as a simple mechanism, the local stiffnesses of which can be determined experimentally, numerically, or more seldom analytically. Specifically, in fracture mechanics, the crack is handled by introducing a so-called flexibility scalar that can be generated from Irwin's relationship between the energy release rate and the stress

0022-460X/90/070115+20 $03.00/0

intensity factor [2]. For example, Rice and Levy [7], Freund and Herrmann [8], and Levy and Herrmann [9] used flexibility scalars and 2×2 flexibility matrices to study the dynamic fracture of beams and plates in bending and stretching. Later, Gudmundson [10] and several other researchers (for example, see reference (11)] generalized this idea to a 6×6 flexibility matrix relating all six generalized forces to the corresponding displacements, and applied it to a variety of dynamic problems.

In the above studies the local flexibility scalars and matrices were formulated from the stress intensity factors of the cracked structures considered. However, these stress intensity factors can be determined analytically or by experimental testing only for simple structures [12]. In general they have to be evaluated by numerical techniques such as the finite element method.

Another important contribution to the analysis of the dynamics of cracked structures is the recent work of Christides and Barr [13], who derived the equation of bending motion for a Bernoulli-Euler beam containing pairs of symmetric open cracks. The cracks were taken to be normal to the beam's neutral axis and symmetrical about the plane of bending (see Figure 1). They used an exponential-type function (the so-called "crack function") to model the stress concentration near the crack tip. The rate of stress decay from the crack was controlled by a dimensionless parameter α that was determined by fitting the analytical results with experimental data. Christides and Barr proposed a two-term Rayleigh-Ritz solution to their equation of motion to evaluate the fundamental natural frequency of a simply supported beam with rectangular cross-section and a pair of mid-span cracks.

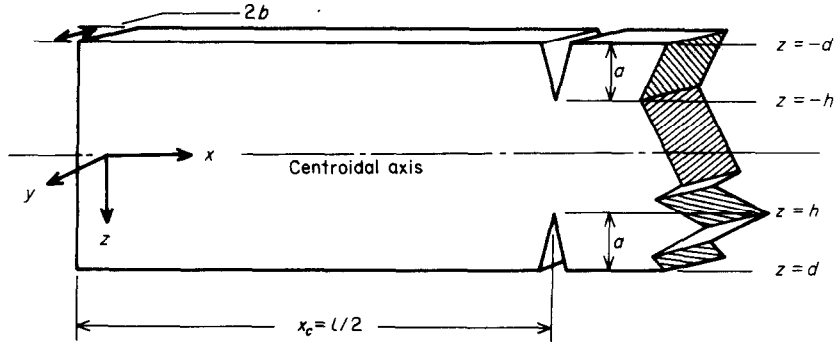

Figure 1. Geometry of simply supported beam with a pair of symmetric cracks at mid-span.

In all the studies mentioned above [3-8] the changes in natural frequencies caused by cracks are determined but the effects on the mode shapes are not considered. However, cracks with different positions and depths could cause nearly the same drop in natural frequency: thus, determining the crack position by vibration monitoring may require the knowledge of the mode shapes as well as that of the frequencies. This demonstrates the importance of calculating the effects of cracks on the mode shapes.

The effects of symmetric cracks on the modes of free vibration of beams in bending are studied in this paper. The cracks are assumed to be always open. The primary objective is to apply the Christides and Barr theory to evaluate accurately the natural frequencies and mode shapes of cracked beams. This is achieved by solving the boundary-value problem by a Galerkin procedure in which the cracked beam deflection is expanded in a series in the eigenfunctions of the corresponding uncracked beam. It is found that the two-term solution proposed by Christides and Barr [13] is not converged and that the convergence of the Galerkin's procedure is indeed very slow for this type of problem.

This leads to a redetermination of the parameter α that controls the stress decay. Also, higher natural frequencies and mode shapes are obtained for the cracked beam. This new Galerkin procedure for the cracked beam problem is presented in section 2. A technique to increase the convergence speed is introduced in section 4, where a function that accounts for the effect of the stress concentration on the continuity characteristics of the exact solution is added to the Galerkin expansion.

In section 3 a finite element calculation of the modes of vibration of cracked beams is presented. Eight-node isoparametric elements model the beam across its thickness. Even though such a crack-tip element is not new and has been widely used in static problems of cracked structures [14-17], the dynamic case requires one to formulate both stiffness and mass matrices and solve the corresponding free vibration eigenvalue problem. The finite element results are found to agree well with the experimental ones of Christides and Barr [13]. An immediate consequence is that the parameter α, which had to be determined from experimental tests, can also be evaluated much less expensively by the finite element method.

2. THEORETICAL FORMULATION

2.1. A BRIEF REVIEW OF CRACKED BEAM THEORY[13]

The assumptions of Christides and Barr for a cracked beam in bending are those of Bernoulli-Euler theory, except that the normal stress and strain are modified to account for the stress concentration near the crack tip. These assumptions are

$$u(x, z, t) = -z\omega'(x, t),\ \varepsilon_{xx}(x, z, t) = [-z + f(x, z)]S(x, t), \qquad \varepsilon_{zz} = -\nu\varepsilon_{xx}, \qquad \varepsilon_{xz} = 0,$$
$$\sigma_{xx}(x, z, t) = [-z + f(x, z)]ES(x, t), \qquad \sigma_{xz} = \sigma_{zz} = 0, \tag{2}$$

where $u(x, z, t)$ and $w(x, t)$ are the displacements in the x and z directions, σ_{xx} and ε_{xx} the stress and strain components in the x direction, and $S(x, t)$ is an unknown strain function. The function $f(x, z)$ was defined in reference [13] as a crack function which is maximum at the crack tip and decays exponentially from the crack along the beam's longitudinal direction:

$$f(x, z) = (z - mz\mathrm{H}(h - |z|)) \exp(-\alpha|x - x_c|/d), \tag{3}$$

where x_c, h and d are the crack position, half the depth of the cracked section, and half the depth of the uncracked section, respectively (see Figure 1). The positive dimensionless constant α determines the rate of stress decay from the crack tip. It cannot be obtained analytically and has to be determined from experimental or finite element results. Note that $f(x, z)$ reduces to z for $|z| > h$ at the cracked section x_c, corresponding to a zero stress. Furthermore, the constant m in the expression of $f(x, z)$ represents the slope of the linear stress distribution in the z direction at the cracked section. The kinematic condition that the same bending moment is carried by both cracked and uncracked beams at the crack tip section yields $m = (d/h)^3$ [13].

Applying the Hu-Washizu variational principle with the strain, stress and displacement assumptions (2), Christides and Barr [13] obtained the following variational expression in terms of the unknowns w and S:

$$\int_{t_1}^{t_2} \left\{ \int_0^l \{[[E(R - I)S]'' - \rho A\ddot{w}]\delta w + E[(I - 2R + L)S - (I - R)w'']\delta S\}\, \mathrm{d}x + \text{boundary terms} \right\} \mathrm{d}t = 0, \tag{4}$$

where $EI(x)$ is the beam's bending stiffness and

$$R = \int_A zf \, dA, \qquad L = \int_A f^2 \, dA. \tag{5}$$

For a beam with rectangular cross-section, R can be easily shown to be equal to zero [13]. Since equation (4) holds for arbitrary admissible variations, it readily yields, for beams with rectangular cross-section

$$S = Q(x)w'', \qquad -(EIS)'' - \rho A\ddot{w} = 0, \tag{6}$$

where

$$Q(x) = I/(I+L) = 1/[1+(m-1)\exp(-2a|x-x_c|/d)]. \tag{7}$$

Thus, the equation of free motion for a beam of rectangular cross-section with symmetric cracks is

$$(EIQw'')'' + \rho A\ddot{w} = 0 \tag{8}$$

with associated boundary conditions. The modes of free vibration are obtained by assuming simple harmonic motion of frequency, ω. Taking $w(x, t) = \hat{w}(x)\,e^{j\omega t}$ leads to the continuous, linear eigenvalue problem with varying coefficients:

$$(EIQ\hat{w}'')'' - \omega^2 \rho A\hat{w} = 0 + \text{boundary conditions}. \tag{9}$$

For an uncracked beam $Q(x)$ reduces to 1 and equation (8) is simply the standard Bernoulli-Euler beam equation. In fact, equation (8) for a cracked beam is that of a "pseudo" Euler-Bernoulli beam with exponentially varying bending stiffness $(EI)^* = EIQ$. Thus, in the Christides and Barr theory, the effect of the crack is simply to modify the bending stiffness, especially in the crack-tip region. Also, the continuity of the solution of equation (9) is altered by the presence of the crack, because the "modified" stiffness EIQ is continuous but has no continuous derivatives (a C^0 function). Therefore one may expect the solution w to be only C^2 in the space variable (continuous up to the second derivative but with a discontinuous third derivative). This can be shown as follows.

From equation (9), $\hat{w}$ continuous implies $(EIQ\hat{w}'')''$ continuous as well. Thus, $EIQ\hat{w}''$ is continuous and since EIQ is continuous so is $\hat{w}''$. In other words, there is continuity of bending moment across the crack (this is indeed one of the original assumptions of Christides and Bar). Also, upon integrating equation (9) once, it follows that $(EIQ\hat{w}'')' = (EIQ)'\hat{w}'' + EIQ\hat{w}'''$ must be continuous. Since $(EIQ)'\hat{w}''$ is discontinuous, this implies that $EIQ\hat{w}'''$ must also be discontinuous as otherwise the sum could not be continuous. This, in turn, requires $\hat{w}'''$ to be discontinuous.

Hence there is a shear discontinuity across the crack. As will be seen in section 4.1, this weaker continuity of the solution in the presence of cracks deteriorates significantly the convergence of the Galerkin procedure.

2.2. A TWO-TERM RAYLEIGH-RITZ SOLUTION [13]

Rayleigh's quotient was used in reference [13] to obtain the drop in the fundamental frequency for a simply supported beam with mid-span cracks ($x_c = l/2$). A two-term expansion of the bending deflection was considered,

$$\hat{w}(x) = \sin(\pi x/l) + \kappa[(x/l) - \tfrac{4}{3}(x/l)^3], \qquad 0 \leqslant x \leqslant l/2, \tag{10}$$

the deflection shape being symmetrical about the $x = l/2$ axis. With the coefficient κ calculated from the stationarity of Rayleigh's quotient, the Christides and Barr solution was found to be in fairly good agreement with the experimental results when the rate of decay was chosen to be $\alpha = 0{\cdot}667$.

2.3. GALERKIN SOLUTION

It is shown in equation (1) that the stress concentration near the crack section effectively reduces the bending stiffness and that the stress is inversely proportional to the square root of the distance to the crack section. However, it is shown in Figure 2 that the normal stress distribution based on the Rayleigh's quotient solution of Christides and Barr [13] neither reaches a maximum at the cracked section nor decays proportionally to $1/\sqrt{r}$. This suggests that convergence is not achieved by assuming a solution in the form of equation (10). Therefore, in this study, the beam deflection is expanded in a series of comparison functions. This not only improves the results as compared to those obtained by Christides and Barr but also predicts the higher natural modes. The deflection of the cracked beam is expanded as

$$\hat{w}(x) = \sum_{i=1}^{N} a_i \phi_i(x), \tag{11}$$

where $\phi_i(x) = \sin(i\pi x/l)$ is the ith mode shape of the corresponding *uncracked* beam, a comparison function, and N is the number of terms in the Galerkin expansion. Substituting equation (11) into equation (9) and applying Galerkin's method yields a discretized eigenvalue problem of size N in the generalized co-ordinates $(a_i)_{i=1,\ldots,N}$,

$$[K_G]\mathbf{a} - \omega^2[M_G]\mathbf{a} = \mathbf{0} \tag{12}$$

where $\mathbf{a} = [a_1, a_2, \ldots, a_N]^T$ is the N-vector of generalized co-ordinates. The mass matrix $[M_G]$ is given by

$$[M_G] = (\rho Al/2)[I], \tag{13}$$

where $[I]$ is the $N \times N$ identity matrix. After a little algebra the stiffness matrix $[K_G]$

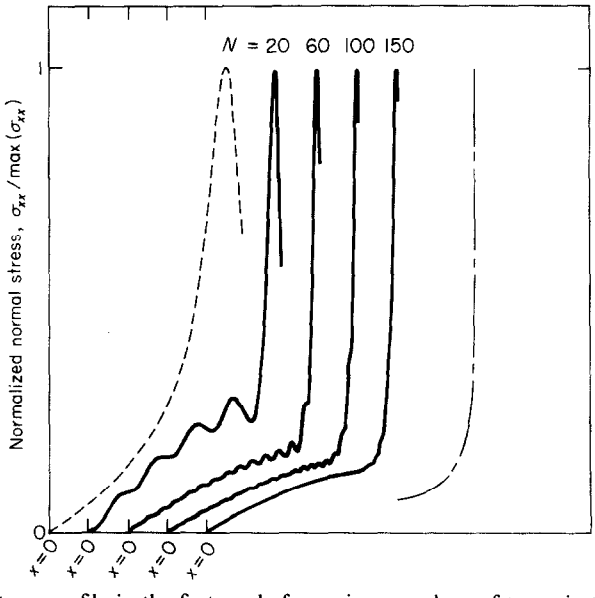

Figure 2. Normal stress profile in the first mode for various numbers of terms in the Galerkin expansion. The beam is simply supported with symmetric cracks at mid-span, for $CR = 1/2$ and $l/2d = 18{\cdot}11$. The origin of each curve is shifted to avoid overlap. Stress profiles are shown from $x = 0$ to $x = l/2$, the crack location. - - -, Christides and Barr [13], $\alpha = 0{\cdot}667$; ———, Galererkin solution, $\alpha = 1{\cdot}936$, $N = 20, 60, 100$ and 150; — - —, $1\sqrt{r}$.

can be shown to be

$$[K_G] = \left(\frac{i\pi}{l}\right)^2 \left(\frac{j\pi}{l}\right)^2 \int_0^l EIQ(x) \sin\left(\frac{i\pi x}{l}\right) \sin\left(\frac{j\pi x}{l}\right) dx. \tag{14}$$

For an uncracked beam $[K_G]$ is obviously diagonal. Because of the expression (7) of $Q(x)$, the integrals in $[K_G]$ cannot be obtained analytically easily and thus a numerical evaluation must be resorted to.

Recall that the function $Q(x)$ depends on the rate of stress decay, α, which cannot be derived from the above theory. Thus, in order to both determine the parameter α and validate the theoretical results, a two-dimensional finite element approach is proposed.

3. FINITE ELEMENT APPROACH

3.1. CRACK-TIP ELEMENT

Henshell and Shaw [14] and Barsoum [15] have demonstrated that, for an eight-node quadrilateral element, by moving the mid-side nodes near the crack tip to the quarterside position (see Figure 3(a)) strain singularities are produced. One can show that this results in a strain singularity of the type $1/\sqrt{r}$ at the crack tip, precisely as required by equation (1). However, for such an element, the singularity conditions prevail only along the edges, and not on an arbitrary ray emanating from the crack tip. Barsoum [16] resolved this problem by collapsing the nodes 1 and 4 of the eight-node quadrilateral element in Figure 3(a), resulting in the triangular element shown in Figure 3(b). Then the singularity prevails on all rays emanating from the crack tip.

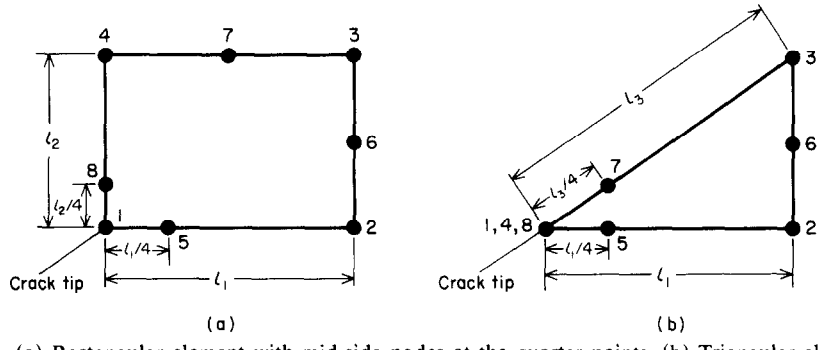

Figure 3. (a) Rectangular element with mid-side nodes at the quarter points. (b) Triangular element with mid-side nodes at the quarter points.

Hibbitt [17] examined closely the properties of singular isoparametric elements that are based on higher-order polynomials. He demonstrated that a singularity of order $r^{(1-n)/n}$ can be obtained with an nth order isoparametric interpolation. He also showed that eight-node quadrilateral elements with side nodes at the quarterside position have unbounded strain energy, and hence stiffness, if the element strain energy is integrated exactly.

According to the assumptions in the Christides and Barr theory, the normal stress distribution on the prospective fracture plane is essentially linear before initiation of the fracture on the tensile side of the beam. This indicates that the quadrilateral quarterpoint element of Figure 3(a) is adequate for the present problem. A nine-point Gaussian integration rule was used in integrating the stiffness matrix, which eliminated the

unbounded strain energy problem mentioned by Hibbitt [17]. However, as a check, all results were also derived using a finite element model composed of triangular quarter-point elements.

3.2. CONSISTENT STIFFNESS AND MASS MATRICES

The assemblage process to generate the system stiffness and mass matrices $[K]$ and $[M]$ is straightforward and results in the free vibration eigenvalue problem for the cracked beam

$$\omega_c^2[M]\mathbf{u} = [K]\mathbf{u}, \tag{15}$$

where $\mathbf{u}$ is the vector of nodal displacements.

4. FREQUENCY AND STRESS CONVERGENCE OF THE GALERKIN PROCEDURE

Upon expanding the cracked beam deflection in the Fourier series (11), the modes of the cracked beam are obtained by solving the eigenvalue problem (12). The approximate solution, however, depends on two key parameters: α, the stress decay constant, and N, the number of terms in the Galerkin expansion. Here the number of terms, N, is first determined by a frequency convergence test. Then the parameter α is estimated by seeking the best match (in a least-squares sense) between the Galerkin solution and finite element and experimental results.

4.1. FREQUENCY CONVERGENCE STUDY

The eigenvalue problem was solved for increasing numbers of terms, N, in the Galerkin expansion until a frequency convergence test was satisfied. The frequency convergence criterion used is

$$E^N = \max_{i=1,2,3} |\Delta\omega_i^N/\omega_i^N| < \varepsilon, \tag{16}$$

where ω_i^N is the N-term estimate of the ith frequency, $\Delta\omega_i^N = \omega_i^N - \omega_i^{N-1}$ is the change in the ith frequency from the $(N-1)$-term to the N-term calculation, and the constant ε is a small real number. For all cases presented, convergence is considered to be achieved when the relative frequency change defined by equation (16) is less than $\varepsilon = 2{\cdot}0 \times 10^{-5}$. Convergence was found to depend very little on the value of the stress decay rate α.

A typical plot of the relative frequency change E^N, versus N is shown in Figure 4 for a simply supported cracked beam with crack depth equal to one-half the beam's thickness. It is observed that the convergence of the Galerkin procedure is very slow, as 150 uncracked modes ($N \geq 150$) are needed in the Galerkin expansion (11) to satisfy the convergence criterion (16). This poor convergence is caused by the discontinuity properties of the coefficients appearing in the continuous eigenvalue problem (9). As noted earlier, the function Q given by equation (7) is slope discontinuous, causing the exact solution $\hat{\omega}$ of the eigenvalue problem (9) to have a discontinuous third derivative. On the other hand, the Galerkin expansion (11) is made of functions that are infinitely differentiable: thus, the Galerkin solution cannot converge to the exact solution in a pointwise fashion. One concludes that using a series of infinitely differentiable functions yields poor convergence because the exact solution is continuous only through its second derivative.

In light of the above information, a significant improvement in convergence can be achieved by introducing an additional, carefully chosen function in the Galerkin expansion. The basic idea is that this supplementary function should have the same

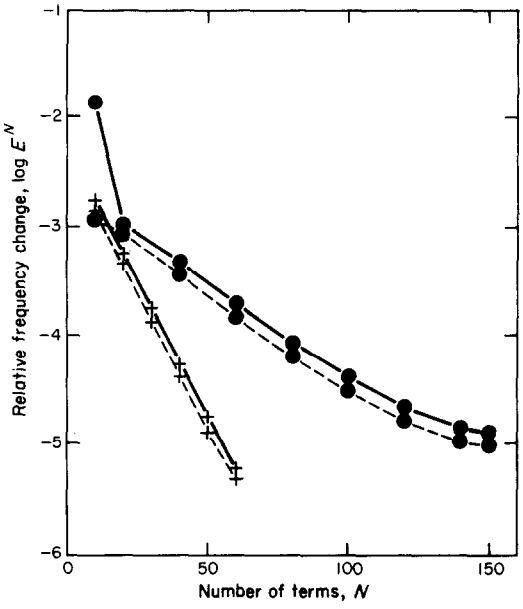

Figure 4. Convergence of the Galerkin procedure for a simply supported beam with a pair of symmetric cracks at mid-span ($CR = 1/2$, $l/2d = 18{\cdot}11$). ●, $N = 10$ to 150 terms; +, one polynomial and $N = 9$ to 59 terms; ——, first mode; - - -, third mode.

continuity properties as the exact solution of the eigenvalue problem. Here the simplest function that is continuous only through its second derivative is a piecewise-defined polynomial of degree three, $\psi(x)$, given by, for mid-span cracks:

$$\psi(x) = \begin{cases} \frac{3}{4}(x/l) - (x/l)^3, & 0 < x \leq l/2 \\ (x/l)^3 - 3(x/l)^2 + \frac{9}{4}(x/l) - \frac{1}{4}, & l/2 < x < l \end{cases}. \tag{17}$$

Such a function can be generated for an arbitrary crack position, x_c. The general form of $\psi_{x_c}(x)$ is given in Appendix A. Thus, the cracked beam deflection is expanded as

$$\hat{\omega}(x) = \sum_{i=1}^{N} a_i \phi_i(x) + a_0 \psi_{x_c}(x). \tag{18}$$

Contrary to the initial expansion (11), the assumed deflection $\hat{\omega}$ in equation (18) satisfies the continuity properties of the exact eigensolution of equation (10), as its second derivative $\hat{\omega}''$ is continuous but its third derivative $\hat{\omega}'''$ is only piecewise continuous with a jump at the crack-tip section. The polynomial (17) was indeed used by Christides and Barr [13] in their two term solution.

The convergence of the series expansion (18) is illustrated in Figure 4. It is shown that convergence is dramatically improved with respect to that of the sine functions expansion when the additional third-order polynomial is included. For example, a 50-term series (consisting of $N = 49$ uncracked modes and one polynomial) is sufficient to satisfy the convergence criterion that required 150 terms when using only infinitely differentiable functions. The reason for this accelerated convergence is that the assumed solution as in equation (18) satisfies the continuity properties of the exact solution. For the rest of the paper, either a 150-term series of the form of equation (11) or a 50-term expansion as in equation (18) had been chosen.

A few remarks are in order. First, using only one additional function that satisfies the continuity characteristics of the exact solution improves drastically the convergence of the Galerkin method, thereby resulting in a substantial reduction in cost. Second, this idea of complementing a Galerkin expansion with one or a few functions that satisfy strictly the continuity requirements of the exact solution is an extension of the work recently published by Gu and Tongue [18]. To accelerate convergence they chose so-called "static modes"— the deflection shapes of the structure under static loading. (A similar idea had been introduced earlier by Kellenberger [19] and Bishop and Parkinson [20] for the problem of flexible rotor balancing.) Indeed, these static modes are usually polynomials that satisfy all the continuity requirements of the exact "dynamic" solution (for a fourth order beam eigenvalue problem, the first static mode is precisely a cubic!). Thus, their approach was essentially equivalent to the one used in this paper. Third, it is believed that this concept can be generalized to all approximate series solutions of partial differential equations, as will be shown by the second author in a future paper. Finally, note that the approach would also apply readily to different boundary conditions.

The convergence of the Galerkin procedure is also indicated by the normal stress profile along the beam. Theoretically, the normal stress should obey a sinusoidal spatial variation, except near the crack where the largest stress concentration should be at the crack tip and the stress should decay proportionally to $1/\sqrt{r}$ from the crack. However, it is shown in Figure 2 that the normal stress distribution based on the Christides and Barr result is not sinusoidal far from the crack, does not have its maximum at the crack tip, and near the crack tip decays at a much smaller rate than $1/\sqrt{r}$. This poor stress profile is yet another indication that their solution is not converged. However, as the number of terms in the Galerkin expansion increases to 60, the maximum stress location moves closer to the crack-tip section and the stress concentration near the crack tip becomes much more pronounced: note, though, the appearance in the profile of high (spatial) frequency oscillations with small amplitudes far from the crack. As the number of terms increases further to 150, these small oscillations superposed to the main profile almost vanish. Furthermore, the maximum stress is located almost at the crack tip, and one can anticipate that if N were increased further the largest stress would be exactly at the tip. Also, there is a very sharp decay in the stress from the crack tip and it is apparent that the stress concentration is governed by a function close to the inverse of the square root of the distance to the crack. Thus, the stress profile for $N = 150$ appears to consist of the sinusoidal variation one would obtain for an uncracked beam with a sharp stress concentration superposed to it near the crack. This indicates that the 150-term solution is nearly fully converged. The stress profile could certainly be improved a little by increasing N, but the additional expense was not deemed necessary.

4.2. DETERMINATION OF THE STRESS DECAY CONSTANT α

Once the number of terms yielding satisfactory convergence is determined, the rate of stress decay α is obtained by fitting the natural frequencies calculated by Galerkin's method best with the finite element results, in a least-squares sense. Even though the first three frequencies were used to determine α, only the fundamental frequency is considered here for simplicity.

The drop in the fundamental natural frequency in terms of crack depth is shown in Figure 5. The least-squares fit between the 150-term Galerkin and the finite element solutions determined the rate of stress decay α to be 1·936. Only crack ratios (the ratio of the crack depth to the half depth of the beam) up to 0·6 were considered in the least squares procedure. Indeed, it is observed in Figure 5 that the agreement between the two techniques is excellent for crack ratios up to 0·65, while the agreement deteriorates for

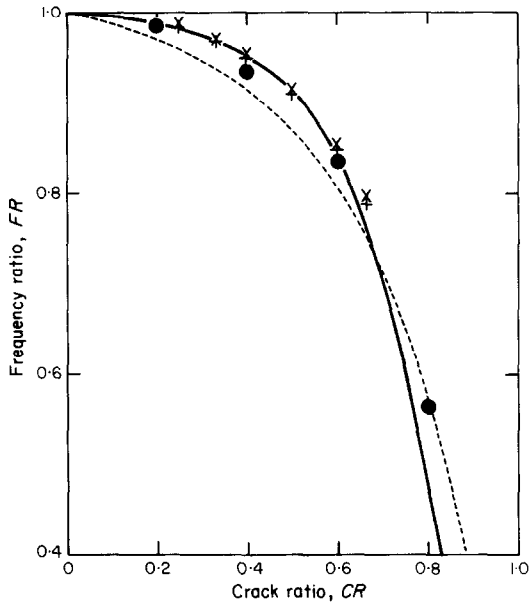

Figure 5. Change in the fundamental natural frequency in terms of crack depth. Theoretical, finite element, and experimental results are shown for a simply supported beam ($l/2d = 18{\cdot}11$) with a pair of symmetric cracks at mid-span. ●, Experiment [13]; +, finite element (rectangular); ×, finite element (triangular; ——, Galerkin solution, $\alpha = 1{\cdot}936$, $N = 150$; - - -, Christides and Barr two-term solution [13], $\alpha = 0{\cdot}667$.

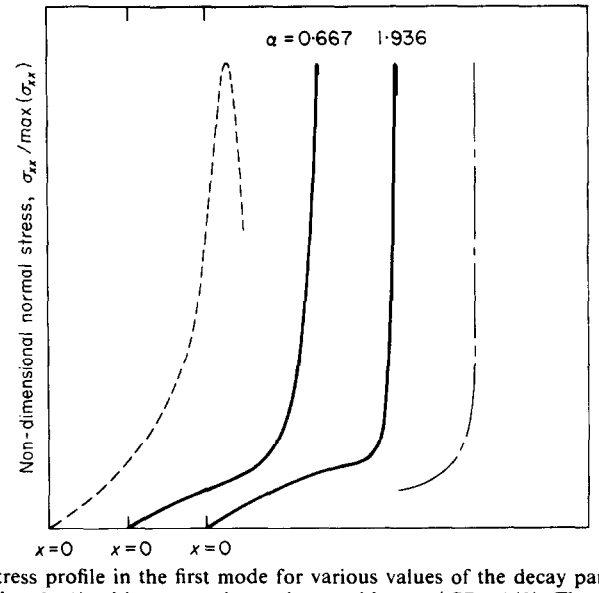

Figure 6. Normal stress profile in the first mode for various values of the decay parameter α, for a simply supported beam ($l/2d = 18{\cdot}11$) with symmetric cracks at mid-span ($CR = 1/2$). The origin of each curve is shifted to avoid overlap. Stress profiles are shown from $x = 0$ to $x = l/2$, the crack location. - - -, Christides and Barr [13], $\alpha = 0{\cdot}667$; ——, Galerkin solution, $N = 150$, $\alpha = 0{\cdot}667$ and $1{\cdot}936$; — - —, $1/\sqrt{r}$.

larger crack ratios. A least-squares procedure that leads to better agreement for very large crack ratios could have been performed, but then a discrepancy would occur for small crack ratios. Thus, the least-squares fit chosen here is believed to be a good compromise because it leads to excellent results for crack ratios up to 0·6, while larger cracks are physically irrelevant since failure would certainly occur long before they can develop. Thus in the rest of the paper the stress decay rate $\alpha = 1{\cdot}936$ is used. Note that it is independent of the crack location and the boundary conditions. Also note that either finite element or experimental tests results can be used to determine α.

It is interesting to note that Christides and Barr [13] determined the rate of stress decay to be $\alpha = 0{\cdot}667$ by fitting their two-term Rayleigh-Ritz solution with experimental data. It is shown in Figure 5 that their solution underestimates all experimental, finite element, and present Galerkin solutions in the zero to 0·6 crack ratio range. Their value of α is believed to be different because it was based on an unconverged two-term solution.

In the previous section it was stated that the stress profile based on the Christides and Barr findings was poor because a two-term expansion was insufficient to achieve convergence. In Figure 6 it is indicated that this is due to their choice for α as well. One notes that the stress profile for 150 terms and $\alpha = 0{\cdot}667$, even though much improved with respect to the two-term profile, does not feature the same sinusoidal-like variation for from the crack and the square root-type concentration near the crack as the $\alpha = 1{\cdot}936$ profile does. Therefore, for a given value of N, the value of the stress decay rate α must be adjusted to achieve both the best stress profile and frequency fit. These observations suggest that sufficient frequency convergence, good agreement with both experimental and finite element results, and excellent normal stress profile are all obtained for $\alpha = 1{\cdot}936$ instead of 0·667 used by Christides and Bar, and for either a 150-term sine function expansion or a 49-term sine function expansion with one third-order polynomial.

5. RESULTS AND DISCUSSION

The modes of free vibration of a simply supported beam with rectangular cross-section and mid-span symmetric cracks have been studied. Results have been obtained for the lowest three natural frequencies and mode shapes in terms of crack depth. Results for the fundamental mode are compared to those of Christides and Barr [13].

5.1. FINITE ELEMENT MESH

The finite element mesh with four quarter-point rectangular elements to model the crack tip is shown in Figure 7(a). This mesh is designed to yield accurate results which rapidly converge as the mesh is refined, both for uncracked and cracked beams. It consists of 40 eight-noded, plane stress, two-dimensional elements, totalling 153 nodal points and 301 degrees of freedom. In Figure 7(a) the beam's slenderness ratio ($\equiv l/2d$) is equal to 18·11. The 16 nodal displacements for each element are the in-plane displacements u and w at each node. The size of the quarter-point elements at the crack tip is chosen to capture the effect of the singularity. The elements cover 1/27·165 of the beam's length in the axial direction, such that they extend over nearly all the stress concentration displayed in Figure 2. Quarter-point elements of various sizes were tested, such that the elements' length was much smaller or much greater than the range of the stress concentration. Too narrow or too wide crack-tip elements led to considerable errors. It was numerically demonstrated that the finite element mesh shown in Figure 7(a) gives a nearly optimal result for the present problem. Since no special procedure is needed to compute the stiffness and mass matrices for the distorted crack tip element, any general-purpose finite element code can be used.

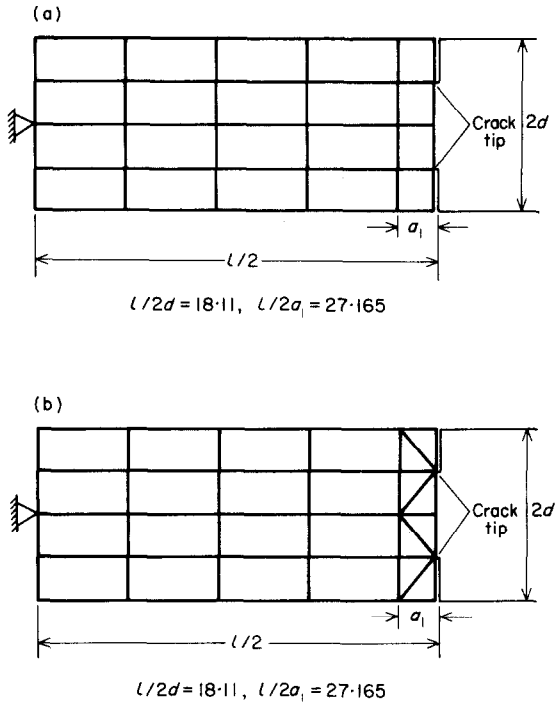

Figure 7. Finite element meshes for simply supported beam with a pair of symmetric cracks at mid-span.

An alternative finite element mesh, which essentially replaces every rectangular quarter-point element in Figure 7(a) by two triangular quarter-point elements, is shown in figure 7(b). The mesh consists of 48 elements, 159 nodal points and 318 degrees of freedom. All the results obtained by the triangular elements are very close to those given by the rectangular ones.

To validate the finite element model, the lowest three natural frequencies of the uncracked beam were compared to Bernoulli-Euler theory results. As shown in Table 1, the finite element frequencies are respectively 0·35, 1·4 and 2·8% lower than the "exact" Bernoulli-Euler ones. Since there are no geometrical assumptions for the finite element formulation, the natural frequencies are expected to be lower, especially for the higher modes.

5.2. NATURAL FREQUENCY RESULTS

The effects of mid-span symmetric cracks on the lower three frequencies are shown in Table 1 and Figures 5 and 8. All results are presented in terms of frequency ratio (FR)—the ratio of the cracked beam frequency to that of the uncracked beam—and crack depth ratio (CR)—the ratio of the depth of the crack to half the beam's thickness. It is shown that the theoretical results agree very well with the finite element calculation for crack ratios up to 0·6. It is also shown in Figure 5 that experimental results for the fundamental mode taken directly from the literature [13] are in good agreement with both finite element and analytical results. On the other hand, the Christides and Barr original solution, which was not fully converged, does not agree as well with either the finite element or the experimental results.

The excessive decrease in frequency predicted by the Galerkin solutions for crack ratios greater than 0·6 might be caused by the assumption made in determining the constant m

TABLE 1

Natural frequencies of uncracked and cracked beams

Uncracked beam (Natural frequency parameter $\beta = \omega_c\sqrt{\rho A l^4/EI}$)

	Fourier representation (150 terms)	Finite element			
		Rectangular		Triangular	
	β	β	*SE*	β	*SE*
1st mode	9·8696	9·8347	1·40934	9·83518	1·40949
2nd mode	39·4784	38·9257	22·30951	38·93774	22·27869
3rd mode	88·8264	86·3489	109·45368	86·39252	109·61885

Cracked beam

Christides and Barr ($\alpha = 0{\cdot}667$)		Fourier representation ($\alpha = 1{\cdot}936$, $N = 150$, $N + N_1 = 49 + 1$)		Finite element			
				Rectangular		Triangular	
CR	*FR*	*FR*	*FR*	*FR*	*SE*	*FR*	*SE*
			First mode				
1/4	0·95803	0·98107	0·98106	0·98284	1·33637	0·98554	1·34650
1/3	0·93685	0·96788	0·96785	0·96618	1·27108	0·96959	1·28323
2/5	0·91353	0·95214	0·95209	0·94788	1·20332	0·95180	1·21694
1/2	0·86924	0·91339	0·91327	0·90787	1·06934	0·91209	1·08458
3/5	0·80577	0·84061	0·84045	0·84563	0·88302	0·85339	0·90406
2/3	0·75120	0·75836	0·75826	0·78646	0·73357	0·79542	0·75447
			Second mode				
1/4	Not available	0·99992	0·99992	1·00033	22·2767	1·00036	22·2802
1/3	Not available	0·99987	0·99987	1·00028	22·2779	1·00032	22·2783
2/5	Not available	0·99979	0·99980	1·00027	22·2774	1·00030	22·2778
1/2	Not available	0·99960	0·99963	1·00026	22·3084	0·99998	22·2784
3/5	Not available	0·99917	0·99925	1·00025	22·2785	1·00031	22·2794
2/3	Not available	0·99853	0·99871	1·00022	22·2790	1·00030	22·2801
			Third mode				
1/4	Not available	0·98179	0·98178	0·98395	97·1274	0·98635	98·1624
1/3	Not available	0·96975	0·96973	0·96875	88·4946	0·97155	89·6094
2/5	Not available	0·95605	0·95600	0·95306	80·9098	0·95615	82·0338
1/2	Not available	0·92514	0·92505	0·92193	68·6454	0·92622	69·8152
3/5	Not available	0·87638	0·87628	0·88072	56·2910	0·88531	57·3790
2/3	Not available	0·83280	0·83275	0·84815	48·6936	0·85263	49·5562

N number of terms in the Galerkin expansion.
N_1, number of special functions.
SE, strain energy.

(which represents the slope of the linear stress distribution at the crack section in z direction). However, as mentioned already, it is impractical to consider such large cracks.

While the effect of cracks on the first and third frequencies, though not large, is noticeable, Table 1 shows that the second natural frequency remains unaffected by cracks of various sizes (even large). This is because the cracks are located at mid-span, where compression and tension vanish for antisymmetrical deflection shapes. Since motion in the second mode is antisymmetrical, the mid-span cracks are not under compression or tension. It follows that the strain in the neutral axis direction is nearly zero (except for a very small in-plane strain due to the in-plane displacement); thus the stress singularity

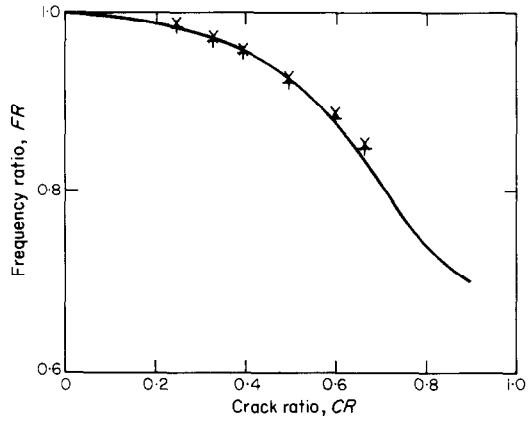

Figure 8. Change in the third natural frequency in terms of crack depth. Theoretical and finite element results are shown for a simply supported beam ($l/2d = 18{\cdot}11$) with a pair of symmetric cracks at mid-span. +, finite element (rectangular); ×, finite element (triangular); ——, Galerkin solution, $\alpha = 1{\cdot}936$, $N = 150$.

vanishes and the second vibration mode is unaffected by the cracks. Indeed, for a beam pinned at both ends, an immediate generalization is that a pair of cracks located at mid-span does not effect any of the antisymmetrical (even) vibration modes.

Since in a number of studies the local flexibility scalars or matrices of cracked structures were formulated from the relationship between the static strain energy release rate and the corresponding crack depth, it is of interest to verify the loss of strain energy, for example by a finite element calculation. It is shown in Table 1 that the strain energy in the first and third modes decreases as the crack size grows, while the strain energy for the second mode, as expected, remains unchanged. This is consistent with the above frequency observations.

It is shown in Table 1 and Figures 5 and 8 that cracks result in a drop in the natural frequencies. However, note that most cracks do not have much of an effect on the beam's frequencies, as cracks half-way through the beam's thickness yield only a 9% reduction in the fundamental frequency. Also, it is rather disappointing to note that the slopes of the curves in Figures 5 and 8 are quite small near the origin, meaning that frequencies have little sensitivity to the presence of small cracks. Therefore, because of parameter uncertainties and measurement errors as well as temperature effects, it appears difficult to utilize only frequency data to monitor and detect the presence of cracks in practical engineering structures such as shafts.

5.3. MODE SHAPE RESULTS

The lowest three mode shapes ae plotted in Figures 9–11 for various crack ratios. Three curves appear on each plot: the present Galerkin result, the finite element approximation and the uncracked beam's mode shape. In addition, the Christides and Barr result for the fundamental mode is shown for comparison. One observes on these plots that the Galerkin result is consistently in better agreement with the finite element mode shape than the Christides and Barr solution is. This is expected and justifies further the convergence observations made in the previous section.

It is shown in Figure 10 that the second mode shape is unaffected by the presence of cracks, for all crack ratios studied. This was predicted above. Moreover, for the first and third modes, the changes in the deflection shapes due to cracks are significant only for crack ratios greater than approximately 1/3. However, note that the third mode shape is more affected by cracks than the first one—see, for example, Figures 9(b) and 11(b).

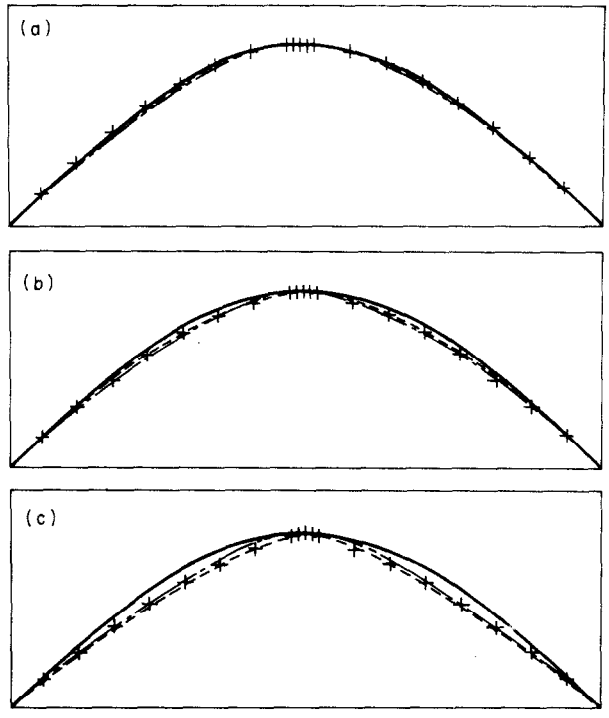

Figure 9. First mode shape of a simply supported beam ($l/2d = 18{\cdot}11$) with a pair of symmetric cracks at mid-span. Galerkin, finite element, and the Christides and Barr results are shown for various crack ratios: (a) $CR = 1/3$; (b) $CR = 1/2$; (c) $CR = 2/3$. +, finite element; - - -, Galerkin solution, $\alpha = 1{\cdot}936$, $N = 150$; - — -, Christides and Barr two-term solution [13]; ——— uncracked beam.

It is also interesting to note that for large crack ratios the deflection shape undergoes a severe change near the crack-tip area. For example, the mode shapes for symmetric cracks penetrating through two-thirds of the beam's thickness are shown in Figures 9(c) and 11(c) they are nearly slope discontinuous at the crack location and resemble those of a beam with a hinge at mid-span. This is also an indication that a large number of uncracked modes are needed in the Galerkin solution to achieve good convergence.

5.4. DISCUSSION

The above results suggest that small symmetric cracks have little effect on the natural frequencies and mode shapes of beams. Only large cracks (crack ratios larger than 0·5) result in moderate frequency and large mode shape changes; unfortunately, structural failure would be likely to occur before such crack sizes are reached.

To estimate crack position and depth from vibration measurement, both frequency and mode shape information should be considered. However, care should be taken in interpreting the results and a multi-mode analysis should be performed. For example, in the case of mid-span cracks, reviewing only the data for the second mode would lead to the erroneous conclusion that the beam is not damaged. Higher mode shapes should probably be considered rather than lower ones, as Figures 9 and 11 show that the third mode is more affected than the first one by cracks. The parameters that reveal a crack's position and depth are the change in frequency, and for the mode shape the abrupt change in slope near the crack tip and the change in the peak amplitudes. On the basis of these ideas, an optimization scheme could be developed to locate cracks from experimental (possibility on-line) data.

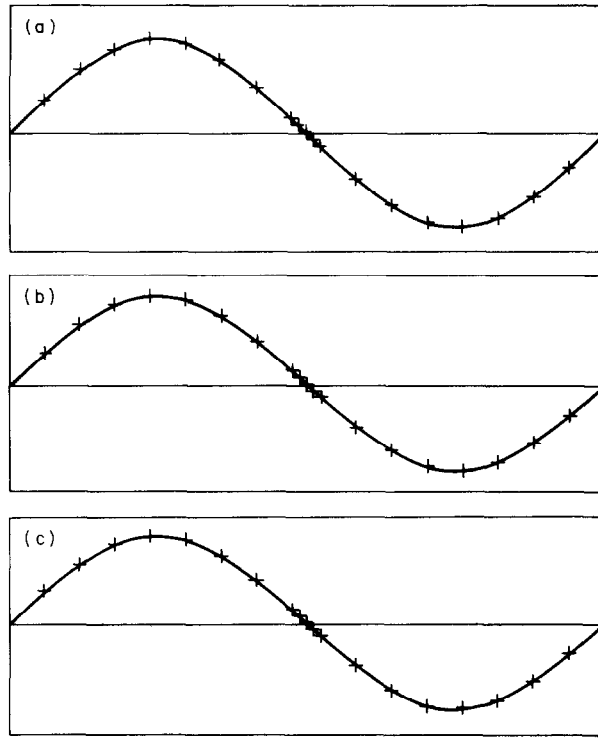

Figure 10. Second mode shape of a simply supported beam ($l/2d = 18{\cdot}11$) with a pair of symmetric cracks at mid-span. Galerkin and finite element results are shown for various crack ratios: (a) $CR = 1/3$; (b) $CR = 1/2$; (c) $CR = 2/3$. Key as Figure 9.

Finally, results were also obtained for a shorter beam with slenderness ratio $l/2d = 10$. The change in frequency versus the crack depth is depicted in Figures 12 and 13. Observe the very good agreement between the two finite element results and the Galerkin solution, especially in the first mode. Also in the first mode, note the poor prediction of the unconverged solution proposed by Christides and Barr. Interestingly, the frequency ratio for this short beam decreases much faster than for the longer beam of Figures 5 and 8 ($l/2d = 18{\cdot}11$) as the crack ratio increases. Thus, the frequencies of short beams appear to be more sensitive to cracks than those of slender beams. This case points out clearly that the proposed converged Galerkin solution provides accurate estimates of the effects of cracks, and that the use of an unconverged solution can yield erroneous results.

6. CONCLUSIONS

A Galerkin-type solution has been proposed for the one-dimensional Bernoulli–Euler equation for a cracked beam that was developed by Christides and Barr. Results for the first three natural frequencies and mode shapes have been shown to agree well with the finite element results presented and the experimental findings of reference [13]. Even though small symmetric cracks were found to have only small effects on the dynamics of beams, the above solution procedure could possibly be applied to determine crack depth and location from frequency and mode shape information: i.e., to solve the inverse problem.

The main drawback of the global Galerkin approach is its slow convergence and the high associated cost. Hence a modified Galerkin expansion that combines the Fourier

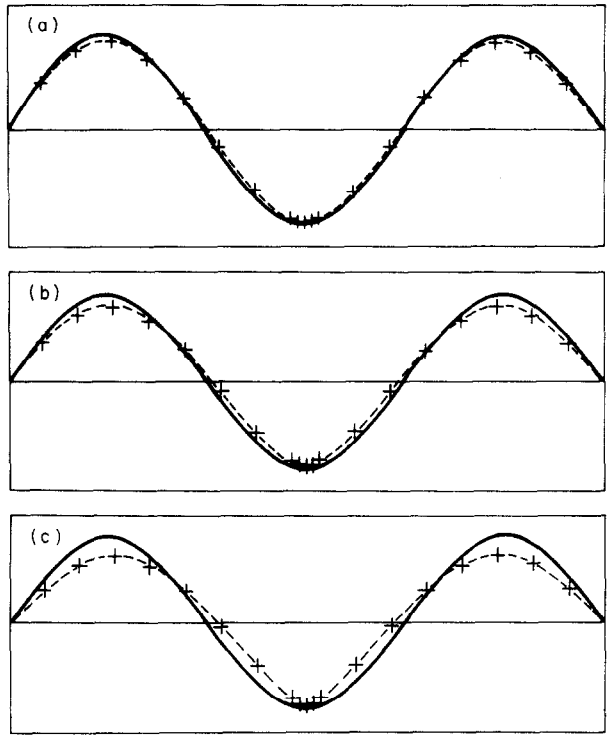

Figure 11. Third mode shape of a simply supported beam ($l/2d = 18{\cdot}11$) with a pair of symmetric cracks at mid-span. Galerkin and finite element results are shown for various crack ratios: (a) $Cr = 1/3$; (b) $CR = 1/2$; (c) $CR = 2/3$. Key as Figure 9.

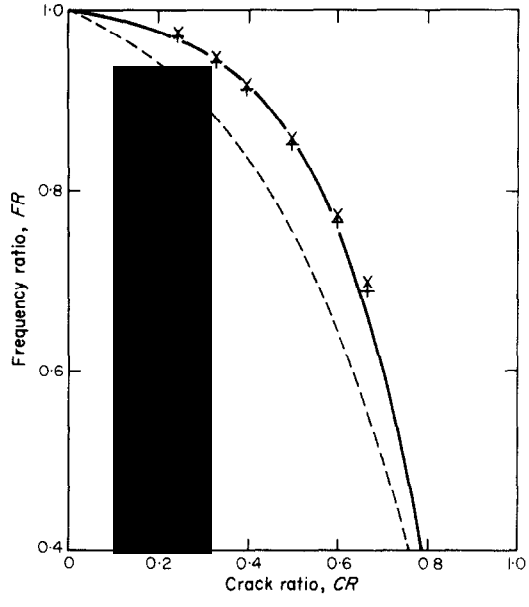

Figure 12. Change in the first natural frequency in terms of crack depth. Theoretical and finite element results are shown for a short simply supported beam ($l/2d = 10$) with a pair of symmetric cracks at mid-span. Key as Figure 5.

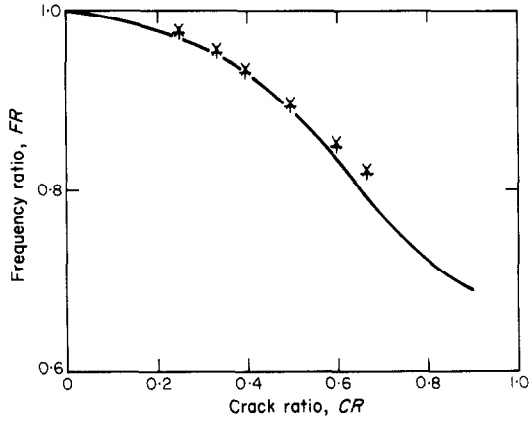

Figure 13. Change in the third natural frequency in terms of crack depth. Theoretical and finite element results are shown for a short simply supported beam ($l/2d = 10$) with a pair of symmetric cracks at mid-span. Key as Figure 8.

series with one additional function satisfying the continuity characteristics of the exact solution has been proposed to improve frequency convergence. An extension of this concept to two or more polynomials could probably be implemented readily. A drastic improvement of the convergence of the Galerkin procedure was observed when using this additional function.

A finite element approach has also been presented that predicts the changes in eigen-frequencies and eigenmodes due to cracks. The use of eight-node singular isoparametric elements to model the crack-tip area resulted in reasonable of the number of degrees of freedom and computational cost.

The parameter α that controls the rate of stress decay previously had to be determined from experimental tests. Here it has been evaluated much less expensively by a finite element approach. This study showed that the value of α should be 1·936 instead of 0·667 suggested by Christides and Barr.

Since, in general, cracks do not occur in symmetric pairs, there is a need for the treatment of the dynamics of beams with *single* cracks. This is to be studied as an extension of the investigation reported here.

ACKNOWLEDGMENTS

This work was partially supported by the Office of the Vice President for Research at the University of Michigan. A Grant No. MSM-8700820 by the National Science Foundation, Dynamic Systems and Control Program, is also acknowledged.

REFERENCES

1. G. R. IRWIN 1960 in *Structural Mechanics* (P. C. Goodier and N. J. Hoff, editors). Oxford: Pergammon Press. See p. 557, Fracture Mechanics section.
2. P. C. PARIS and G. C. SIH 1965 *Fracture Toughness and its Applications.* ASME STP- **381**, 30. Stress analysis of cracks.
3. I. IMAN, J. SCHEIHEL, S. H. AZZARO and R. J. BANKERT 1987 *The* 1987 *ASME Design Technology Conference, Rotating Machinery Dynamics* **2**, 615-629. Development of an on-line rotor crack detection and monitoring system.
4. I. W. MAYES and W. G. R. DAVIES 1976 *Conference on Vibrations in Rotating Machinery* (*IME Conference*) C168/76 53-64. The vibrational behaviour of a rotating shaft system containing a transverse crack.

5. T. A. HENRY and B. E. OKAH-AVAE 1976 *Conference on Vibrations in Rotating Machinery (IME Conference)* C162/76 15-19. Vibration in cracked shaft.
6. I. W. MAYES and W. G. R. DAVIES 1984 *Journal of Vibration, Acoustics, Stress, and Reliability in Design, Transactions of the American Society of Mechanical Engineers* **106**, 139-145. Analysis of the response of a multi-rotor-bearing system containing a transverse crack in a rotor.
7. J. R. RICE and N. LEVY 1975 *Journal of Applied Mechanics, Transactions of the American Society of Mechanical Engineers* **97**, series E, 435-439. The part-through surface crack in an elastic plate.
8. L. B. FREUND and G. HERRMANN 1975 *Journal of Applied Mechanics, Transactions of the American Society of Mechanical Engineers* **43**, 112-116. Dynamic fracture of a beam or plate in pure bending.
9. C. LEVY and G. HERRMANN 1982 *Journal of Applied Mechanics, Transactions of the American Society of Mechanical Engineers* **49**, 656-658. On the effect of axial force in dynamic fracture of a beam or a plate in pure bending.
10. P. GUDMUNDSON 1983 *Journal of the Mechanics and Physics of Solids* **31** (4), 329-345. The dynamic behaviour of slender structures with cross-sectional cracks.
11. C. A. PAPADOPOULOS and A. D. DIMAROGONAS 1987 *Ingenieur-Archiv* **57**, 257-266. Coupling of bending and torsional vibration of a cracked Timoshenko shaft.
12. H. TADA, P. PARIS and G. IRWIN 1973 *The Stress Analysis of Cracks Handbook.* Hellertown, Pennsylvania: Del Research Corporation.
13. S. CHRISTIDES and A. D. S. BARR 1984 *International Journal of the Mechanical Sciences* **26** (11/12), 639-648. One-dimensional theory of cracked Bernoulli-Euler beams.
14. R. D. HENSHELL and K. G. SHAW 1975 *International Journal of Numerical Methods in Engineering* **9**, 495-509. Crack tip finite element are unnecessary.
15. R. S. BARSOUM 1976 *International Journal of Numerical Methods in Mngineering* **10**, 23-37. On the use of isoparametric finite element in linear fracture mechanics.
16. R. S. BARSOUM 1977 *International Journal of Numerical Methods in Engineering* **11**, 85-98. Triangular quarter point elements as elastic and perfectly-plastic crack tip elements.
17. H. D. HIBBITT 1977 *International Journal of Numerical Methods in Engineering* **11**, 180-184. Some properties of singular isoparametric elements.
18. K. GU and B. H. TONGUE 1987 *Journal of Applied Mechanics, Transactions of the American Society of Mechanical Engineers* **54**, 904-909. A method to improve the modal convergence for structures wth external Forcing.
19. W. KELLENBERGER 1972 *Journal of Engineering for Industry, Transactions of the American Society of Mechanical Engineers* **94**, 548-560. Should a flexible rotor be balanced in N or $(N+2)$ planes?
20. R. E. D. BISHOP and A. G. PARKINSON 1972 *Journal of Engineering for Industry, Transactions of the American Society of Mechanical Engineers* **94**, 561-576. On the use of balancing machines for flexible rotors.

APPENDIX A

$$\psi_{x_c}(x) = \begin{cases} [(x_c/l)^2 - 3(x_c/l) + 2](x/l) + [1 - 1/(x_c/l)](x/l)^3, & 0 < x \leqslant x_c \\ (x/l)^3 - 3(x/l)^2 + [2 + (x_c/l)^2](x/l) - (x_c/l)^2, & x_c < x < l \end{cases}.$$

APPENDIX B: NOMENCLATURE

a	crack depth
a_i	ith generalized co-ordinate amplitude
A	cross-sectional area
b	half breadth of rectangular beam
CR	$\equiv a/d$, crack ratio
d	half depth of rectangular beam
E	Young's modulus
$f(x, z)$	crack function
h	$\equiv d - a$
$\mathrm{H}(\cdot)$	unit step function
I	cross-sectional area moment of inertia

$[K]$	global stiffness matrix (finite element)
$[K_G]$	stiffness matrix (Galerkin's method)
l	length of beam
$Q(x)$	integrated crack function
m	stress magnification factor
$[M]$	global mass matrix (finite element)
$[M_G]$	mass matrix (Galerkin's method)
N	number of terms in Galerkin expansion
r	distance from the crack tip
$S(x, t)$	strain function
$w(x, t)$	bending displacement
$\hat{\omega}(x)$	displacement amplitude
x	distance along beam
x_c	crack position
α	stress decay constant
δ_{ij}	Kronecker's delta, $=1$ for $i=j$ and $=0$ for $i \neq j$
ρ	density
ε_{ij}	strain tensor component
σ_{ij}	stress tensor component
$\phi_i(x)$	ith mode shape of uncracked beam
ω	free vibration natural frequency
$(\cdot)$	$\equiv \partial/\partial t$
$(')$	$\equiv \partial/\partial x$